Available online at www.sciencedirect.com
SCIENCE DIRECT®
Journal of Chromatography A, 1091 (2005) 60–71
JOURNAL OF CHROMATOGRAPHY A
www.elsevier.com/locate/chroma

Analysis of sample–solvent induced modifier–solute peak interactions in biochromatography using equilibrium theory and detailed simulations

Guido Ströhlein [a], Marco Mazzotti [b], Massimo Morbidelli [a,*]

[a] *Swiss Federal Institute of Technology, ETHZ, Institut für Chemie and Bioingenieurwissenschaften, ETH-Hönggerberg/HCI, CH-8093 Zurich, Switzerland*
[b] *Swiss Federal Institute of Technology, ETHZ, Institute of Process Engineering, Sonneggstrasse 3, CH-8092 Zurich, Switzerland*

Received 18 February 2005; received in revised form 6 July 2005; accepted 11 July 2005
Available online 8 August 2005

Abstract

Batch liquid chromatographic columns are often equilibrated with an eluent stream being a mixture of inert compounds and so-called modifiers. The sample injected into the eluent stream usually consists of the solutes to be separated and of a mixture of the same solvents as in the eluent but in general with different concentration values. This results in two groups of peaks moving along the column: the solute peaks and the modifier pertubations. If the adsorptivity of the solute depends strongly on the modifier, as it is often the case in biochromatography, the interference between the two groups of peaks leads to peculiar phenomena like double peaks, split peaks, distorted peaks with anti-Langmurian shape, etc. In this work, these phenomena are analyzed based on an analytical solution of the equilibrium theory model and the results are compared with detailed simulations and experimental data. It is shown that the qualitative behavior is well predicted in the frame of equilibrium theory and general guidelines how to avoid these kinds of interactions are developed.

Keywords: Biochromatography; Equilibrium theory; Sample–solvent; Double peaks

1. Introduction

Batch liquid chromatographic columns are typically equilibrated with an eluent stream which contains a mixture of two, or more, components which can adsorb more or less on the stationary phase and are used to tune the adsorption behavior of the solutes to be separated. The sample injected into the eluent stream consists of the solutes to be separated, and of a mixture of the same solvents as in the eluent but in general with different concentration values. The interaction between the solutes, the stationary phase and the eluent components can lead to complex and intriguing phenomena that have always attracted the attention of chromatographers.

A typical example is offered by the so-called system peaks and the related phenomena like extra peaks and peak deformation which have been investigated thoroughly by Guiochon and co-workers [1–3]. System peaks occur when an eluent is made up of at least two different compounds with at least one adsorbing species and when the injected solute affects the solid phase concentration of the adsorbing eluent species. In this case, due to the adsorption of the solute, the solid phase equilibrium concentration of the adsorbing eluent species is perturbed. Consequently, two different kinds of peaks migrate along the column: one due to the injected solute and one due to the eluent species displaced in the solid phase. The latter ones are called system peaks. It should be noted that system peaks can also occur when the concentration of the adsorbing species in the eluent stream is the same as in the sample injection.

Due to the sample–solvent interaction, a different class of phenomena occurs when the concentrations of the adsorbing eluents (i.e. the so-called modifiers) in the injected sample are different from the ones in the eluent stream. The migration of this positive or negative perturbation of the modifier concentration can strongly affect the retention time of the

* Corresponding author. Tel.: +41 16323034; fax: +41 16321082.
E-mail address: morbidelli@tech.chem.ethz.ch (M. Morbidelli).

0021-9673/$ – see front matter © 2005 Elsevier B.V. All rights reserved.
doi:10.1016/j.chroma.2005.07.035

solute. This is seen particularly in biochromatography where the adsorption of the solute, e.g. a peptide or a protein, is strongly dependent on the modifier concentration, such as an organic solvent or an inorganic salt. System peaks might also occur in this case if the adsorption of the solute affects the modifier concentration in the solid phase, thus adding another dimension of complexity to the phenomenon.

In this work we consider the phenomena induced by the sample–solvent in the case where the solute is injected highly diluted while the modifier concentration in the mobile phase is sufficiently large to enter the non-linear region of its adsorption isotherm. These are typical conditions encountered, for example, when one wants to estimate the Henry constant of the solute as a function of the eluent phase composition by measuring the retention time of a highly diluted peak of the solute. The question is whether sample–solvent phenomena can affect such retention times, thus masking the correct Henry constant values. It is clear that under these conditions system peaks do not occur, since the solute is too dilute to alter the concentration of the species in the mobile phase.

These processes have been studied in the context of bio [4] and fine chemical [5–7] chromatography, either adopting a qualitative interpretation of the phenomena observed experimentally or running simulation using detailed models. In this work, it is shown that these phenomena can be described, understood and predicted using a simple analytical model which is based on existing solutions of the equilibrium theory model. This model provides general and quantitative predictions of the conditions where double peaks, distorted peaks and severe alteration of the observed retention time occur due to the strong interactions between the modifier perturbation and the solute peak. It has to be kept in mind that quantitative predictions would require a detailed knowledge of the isotherms.

Finally, a simple representation of the operating condition space is proposed, where general guidelines how sample–solvent induced phenomena can be avoided are given.

It has to be noted that having a sample solvent with the same composition as the eluent allows avoiding a local perturbation of the modifier concentration and the consequent phenomena mentioned above. However, it is often difficult for practical reasons to adjust the sample solvent to the eluent composition.

2. Equilibrium theory model

The equilibrium theory of chromatography assumes that the liquid and the solid phase are at every time and position in the column at equilibrium and that axial dispersion is negligible, i.e. infinite column efficiency.

These assumptions are fairly well fulfilled in many chromatographic applications. When considering one-dimensional flow (no radial gradient) and a constant fluid flow velocity, the mass balance over an infinitely small column element yields [8]

$$\varepsilon^* \frac{\partial c_i}{\partial t} + (1-\varepsilon^*)\frac{\partial q_i}{\partial t} + u\frac{\partial c_i}{\partial z} = 0 \tag{1}$$

being ε^* the total column porosity, c_i and q_i the liquid and solid phase concentration, respectively, t the time, z the space coordinate and u the superficial velocity.

Eq. (1), together with the equilibrium isotherm $q_i = f(c_i)$ is a set of reducible, first-order PDEs whose solution has been discussed in detail by Rhee et al. for the single-component [9] as well as for the multi-component case [10]. In the following, we consider the solution of this model for one modifier and one solute in the cases where the modifier exhibits a linear or a Langmuir isotherm, whereas the solute, being highly diluted, exhibits a linear isotherm in both cases. In addition, following the typical experimental behavior, we assume that the adsorption isotherm of the modifier is not affected by the solute, while the Henry constant of the latter is a strong function of the modifier concentration.

2.1. Linear isotherm for the modifier

Let us consider the mass balance of Eq. (1) for both the modifier and the solute in the case of a linear modifier isotherm, i.e.

$$q_\mathrm{M} = H_\mathrm{M} c_\mathrm{M} \tag{2}$$

whereas the adsorption of the solute depends on the modifier concentration according to:

$$q_\mathrm{S} = H_\mathrm{S}(c_\mathrm{M}) c_\mathrm{S} \tag{3}$$

Substituting these two isotherms into Eq. (1) yields the pair of PDEs

$$\frac{\partial c_\mathrm{M}}{\partial x} + (1+\nu^* H_\mathrm{M})\frac{\partial c_\mathrm{M}}{\partial \tau} = 0 \tag{4}$$

$$\frac{\partial c_\mathrm{S}}{\partial x} + (1+\nu^* H_\mathrm{S}(c_\mathrm{M}))\frac{\partial c_\mathrm{S}}{\partial \tau} + \nu^* c_\mathrm{S}\frac{\mathrm{d}H_\mathrm{S}(c_\mathrm{M})}{\mathrm{d}c_\mathrm{M}}\frac{\partial c_\mathrm{M}}{\partial \tau} = 0 \tag{5}$$

where $x = z/L$, $\tau = ut/(L\varepsilon^*)$ and the phase ratio is defined as $\nu^* = (1-\varepsilon^*)/\varepsilon^*$. The boundary and initial conditions for an injected pulse of the solute and the modifier into an eluent stream containing only the modifier at a different concentration are given by:

$$\begin{aligned} &0 \le \tau \le \tau_\mathrm{Inj}: \quad c_\mathrm{M}(x=0,\tau) = c_\mathrm{M}^\mathrm{Inj}; \quad c_\mathrm{S}(x=0,\tau) = c_\mathrm{S}^\mathrm{Inj} \\ &\tau > \tau_\mathrm{Inj}: \quad c_\mathrm{M}(x=0,\tau) = c_\mathrm{M}^0; \quad c_\mathrm{S}(x=0,\tau) = 0 \end{aligned} \tag{6}$$

$$\begin{aligned} c_\mathrm{M}(x,\tau=0) &= c_\mathrm{M}^0 \\ c_\mathrm{S}(x,\tau=0) &= 0 \end{aligned} \tag{7}$$

Exploiting the feature that Eq. (5) depends on the solution of Eq. (4) but not vice versa, the solution of Eq. (4) can be easily represented in the physical plane using the method of characteristics [9,10]. The characteristics are lines, straight

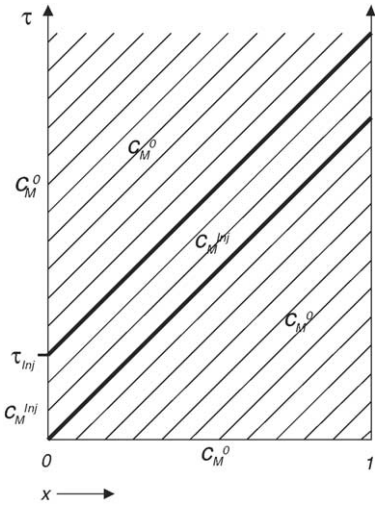

Fig. 1. Modifier characteristics in the case of linear modifier adsorption isotherm.

in this case, that propagate a concentration value from where it is assigned, as either boundary ($x = 0$) or initial ($\tau = 0$) condition, into the physical plane (x, τ). For a linear isotherm, the migration velocity of a component is independent of its concentration and therefore the characteristics of the modifier are the straight, parallel lines shown in Fig. 1, whose slope is σ_M:

$$\sigma_M = 1 + \nu^* H_M \tag{8}$$

The inlet perturbation of the eluent concentration from c_M^0 to c_M^{Inj} travels as a rectangle through the column, so that the modifier concentration as a function of time and position in the column is given by:

$$c_M(x,\tau) = \begin{cases} c_M^0 & \sigma_M x > \tau \\ c_M^{Inj} & \sigma_M x + \tau_{Inj} > \tau > \sigma_M x \\ c_M^0 & \tau > \sigma_M x + \tau_{Inj} \end{cases} \tag{9}$$

The solution of the solute mass balance (Eq. (5)) can be obtained by considering that the term $\partial c_M/\partial\tau = 0$ in the entire integration plane with the exception of the straight lines $\tau = \sigma_M x$ and $\tau = \sigma_M x + \tau_{Inj}$ where it is not defined. If we integrate Eq. (5) separately in the three different regions shown in Fig. 1, we find that also the solute concentration propagates along straight characteristics whose slopes in the three different c_M-domains are given by:

$$\sigma_S(x,\tau) = \begin{cases} 1 + \nu^* H_S(c_M^0) & \sigma_M x > \tau \\ 1 + \nu^* H_S(c_M^{Inj}) & \sigma_M x + \tau_{Inj} > \tau > \sigma_M x \\ 1 + \nu^* H_S(c_M^0) & \tau > \sigma_M x + \tau_{Inj} \end{cases} \tag{10}$$

With these expressions, the propagation of the injected solute pulse can easily be calculated.

In the following, three cases are discussed in order to provide an introductory example for understanding the effect of sample–solvent phenomena. In particular, we consider

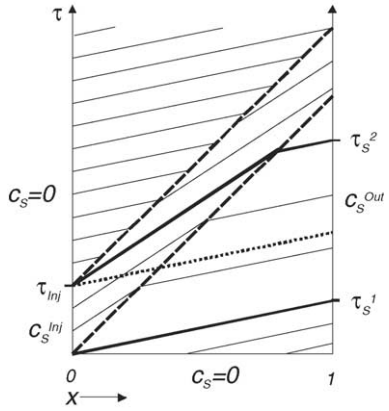

Fig. 2. Case (a), dashed lines: modifier characteristics enclosing injected peak; solid lines: solute characteristics; dotted line: isocratic solute characteristic.

the following typical experimental conditions, namely that $H_S(c_M)$ is a strongly monotonically decreasing function and that a vacancy modifier peak with $c_M^{Inj} < c_M^0$ is injected. This implies that the solute travels faster outside the modifier peak than inside it, since $H_S(c_M^{Inj}) > H_S(c_M^0)$. In this case, the following three situations can occur, depending upon the relative value of the modifier Henry constant, H_M:

(a) $H_M > H_S(c_M^{Inj}) > H_S(c_M^0)$
(b) $H_S(c_M^{Inj}) > H_S(c_M^0) > H_M$
(c) $H_S(c_M^{Inj}) > H_M > H_S(c_M^0)$

In case (a), the vacancy peak of the modifier travels slower than the solute both inside and outside the modifier peak. Therefore, the solute peak travels to the front of the modifier peak, leaves it and enters the domain with a higher modifier concentration ($c_M^{Inj} < c_M^0$), where it further accelerates. The characteristic lines corresponding to this case are shown in Fig. 2. It is seen that, when compared with the isocratic peak, the solute peak is retarded and broadened by the interaction with the modifier peak. By isocratic peak we mean the solute peak that one would obtain if the modifier concentration was c_M^0 in the entire column. This is the situation illustrated by the dotted characteristic line in Fig. 2, while the real and isocratic peaks are shown in Fig. 3.

It is worth noting that the solute concentration along its characteristic is not constant in this case due to the change in the migration velocity when leaving the modifier peak. The solute concentration in fact decreases and its value in the

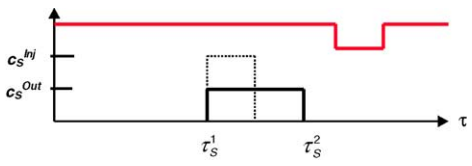

Fig. 3. Case (a), solid lines: modifier and solute chromatogram; dotted line: isocratic solute chromatogram.

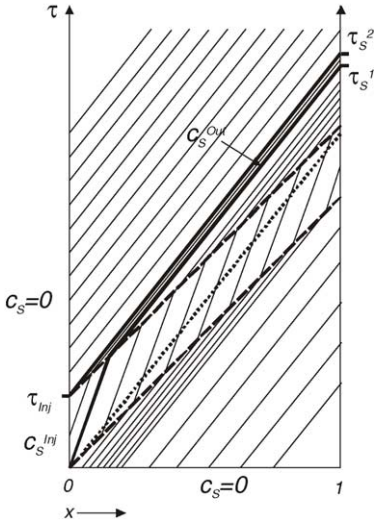

Fig. 4. Case (b), dashed lines: modifier characteristics enclosing injected peak; solid lines: solute characteristics; dotted line: isocratic solute characteristic.

solute peak at the column outlet is given by:

$$c_S^{Out} = \frac{H_M - H_S(c_M^{Inj})}{H_M - H_S(c_M^0)} c_S^{Inj} \quad (11)$$

which indicates that the peak broadening is larger the larger the difference between c_M^0 and c_M^{Inj} is, whereas the breakthrough times of the front and the rear part of the peak are given by

$$\tau_S^1 = 1 + \nu^* H_S(c_M^0) \quad (12)$$

$$\tau_S^2 = 1 + \nu^* H_S(c_M^0) + \tau_{inj} \frac{H_M - H_S(c_M^0)}{H_M - H_S(c_M^{Inj})} \quad (13)$$

In case (b), the modifier vacancy peak travels faster than the solute both inside and outside the modifier peak. Therefore the solute crosses the rear boundary of the modifier peak and enters the region of higher modifier concentration, where it accelerates. As shown in Fig. 4, this leads to the sharpening of the eluted peak, which is also retarded with respect to the isocratic peak, as shown in Fig. 5.

The solute concentration in the outlet peak is again given by Eq. (11), but it is now larger than in the injected peak since the multiplier of c_S^{Inj} in Eq. (11) is bigger than 1.

For case (c), the migration velocity of the modifier peak is larger than that of the solute inside the modifier peak but smaller outside. Hence, the solute characteristics intersect

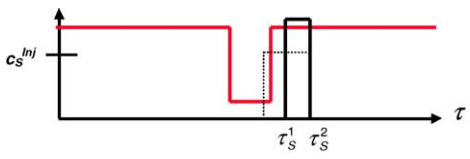

Fig. 5. Case (b), solid lines: modifier and solute chromatogram; dotted line: isocratic solute chromatogram.

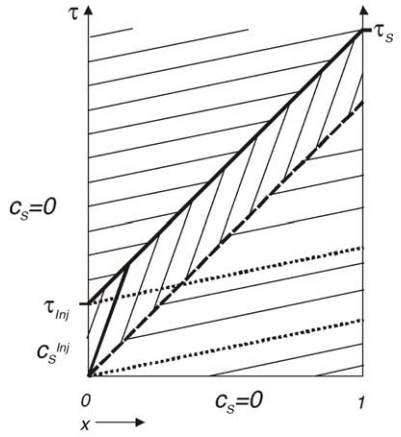

Fig. 6. Case (c), dashed lines: modifier characteristics enclosing injected peak; solid lines: solute characteristics; dotted line: isocratic solute characteristic.

the rear boundary of the modifier peak. If the solute enters the domain behind the vacancy modifier peak, i.e. where c_M^0 prevails, it will travel faster than the modifier peak itself, hence it will re-enter the modifier peak from behind where it will be slowed down again. As a consequence, the solute is confined at the end of the modifier peak, propagates with the rear end of the modifier peak and is finally eluted as a very sharp peak as shown in Figs. 6 and 7. It is worth noting that in this case the solute peak is narrow, but its retention time is determined by the Henry constant of the modifier and the injection time, and not by the Henry constant of the solute. This would obviously create a problem when estimating the solute Henry constants from its retention times.

The peculiar chromatographic behavior as discussed above for the three cases has also been analyzed in the hodograph plane, yielding the same results and, due to the mathematically more stringent argumentation, further insight into the phenomena [11].

In the context of the above discussion it is worth mentioning that the system behavior would become more complex if we account for some simple dispersive effect. Assuming an injection with a slightly dispersed solute and modifier peak front, the solute molecules at the peak front find themselves in an environment with a higher modifier concentration than in the injection pulse due to the dispersion effect. If this modifier concentration is large enough, the solute molecules travel faster than the modifier peak and elute with a retention time determined by $H_S(c_M^0)$, whereas the main fraction of the solute molecules travels to the rear of the modifier vacancy

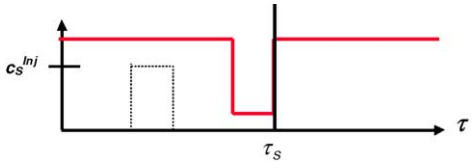

Fig. 7. Case (c), solid lines: modifier and solute chromatogram; dotted line: isocratic solute chromatogram.

peak and elutes with a retention time determined by H_M as discussed with reference to Fig. 6. In this case, two distinct solute peaks would occur in the chromatogram originated by the injection of a single solute, as discussed later in detail.

2.2. Langmuir adsorption isotherm for the modifier

Let us now consider the case where the modifier exhibits a Langmuir adsorption isotherm:

$$q_M(c_M) = \frac{H_M c_M}{1 + K_M c_M} \tag{14}$$

The mass balance equation for the solute (Eq. (5)) and its isotherm (Eq. (3)) remain unchanged.

Due to the non-linearity of the modifier isotherm, the characteristic lines for the modifier are not parallel lines as in the linear case. Their local slope is actually a function of the concentration c_M, according to the relationship:

$$\sigma_M(c_M) = 1 + \nu^* \frac{H_M}{(1 + K_M c_M)^2} \tag{15}$$

The propagation behavior of the modifier along the column is well known [9], and in the case of a vacancy peak the modifier step propagates through a dispersive wave in the front and a shock in the rear. If the injected volume is small in comparison to the column volume, the rear shock catches up the front wave before the column outlet, and the wave and the shock interact as illustrated in Fig. 8.

The characteristic lines for the modifier for an injection $c_M^{Inj} < c_M^0$ are shown in Fig. 8.

Similarly to the linear case, in the regions above line F–A–C and below line 0–B the modifier concentration is constant and equal to c_M^0. The rear end of the peak, represented by the line F–A–C, travels as a shock with a concentration jump from c_M^{Inj} to c_M^0 along line F–A, while the concentration change through the discontinuity line A–C monotonically decreases as the concentration on the right hand side of it increases from A to C. The triangle 0–A–F represents a plateau, where the modifier concentration is equal to c_M^{Inj}.

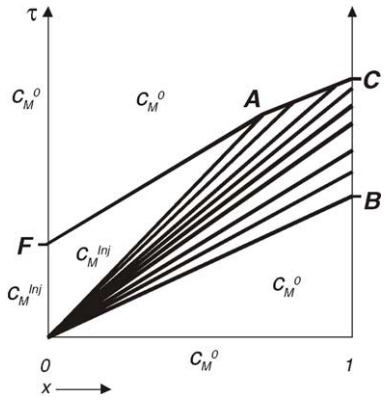

Fig. 8. Modifier characteristics for negative perturbation, Langmuir isotherm.

The front part of the peak consists of a dispersive wave which broadens along the column. Each line in the dispersive wave region 0–A–C–B is the characteristic corresponding to a specific modifier concentration according to Eq. (15).

The slope of the line 0–A is given by Eq. (15) as:

$$\sigma_M^{0-A}(c_M^{Inj}) = 1 + \nu^* \frac{H_M}{(1 + K_M c_M^{Inj})^2} \tag{16}$$

while the slope of the shock along line F–A is given by

$$\sigma_M^{F-A}(c_M^0, c_M^{Inj}) = 1 + \nu^* \frac{H_M}{(1 + K_M c_M^0)(1 + K_M c_M^{Inj})} \tag{17}$$

hence $\sigma_M^{F-A} < \sigma_M^{0-A}$.

The line A–C is not a straight line and its behavior is described by

$$\tau_{A-C} = x + \left(\frac{\sqrt{\nu^* H_M}}{1 + c_M^0 K_M} (\sqrt{x} - \sqrt{x_A}) + \sqrt{\tau_A - x_A} \right)^2 \tag{18}$$

where the coordinates x_A and τ_A of point A are given by

$$x_A = \frac{(1 + c_M^0 K_M)(1 + c_M^{Inj} K_M)^2 \tau_{Inj}}{(c_M^0 - c_M^{Inj}) H_M K_M \nu^*} \tag{19}$$

$$\tau_A = \sigma_M^{0-A} x_A \tag{20}$$

The interaction between the modifier and the solute peak depends strongly on the slope of the solute characteristics at c_M^{Inj}, which prevails in the triangle 0–A–F. This slope is simply given by

$$\sigma_S(c_M^{Inj}) = 1 + \nu^* H_S(c_M^{Inj}) \tag{21}$$

Now, we can have the following three possibilities as far as the slope of the solute characteristics at c_M^{Inj} is concerned:

(a) it is lower than the slope of the shock characteristic, i.e. $\sigma_S(c_M^{Inj}) < \sigma_M^{F-A}$, and the solute travels towards the front of the plateau and intersects line 0–A.
(b) it is higher than the slope of line 0–A, i.e. $\sigma_S(c_M^{Inj}) > \sigma_M^{0-A}$, and the solute travels to the rear of the plateau, i.e. line F–A.
(c) it is intermediate between the slope of F–A and of 0–A, i.e. $\sigma_M^{0-A} > \sigma_S(c_M^{Inj}) > \sigma_M^{F-A}$, and some of the characteristics intersect line F–A, whereas others intersect line 0–A.

In case (a), the solute characteristics cross line 0–A, and then intersect characteristics with higher c_M. Therefore, H_S decreases, and so do the slopes of the characteristics. Subsequently, the solute leaves the dispersive wave, and then travels with a velocity corresponding to $H_S(c_M^0)$. The path through the wave region can be calculated by integrating the local slopes of the solute characteristics given by Eq. (22).

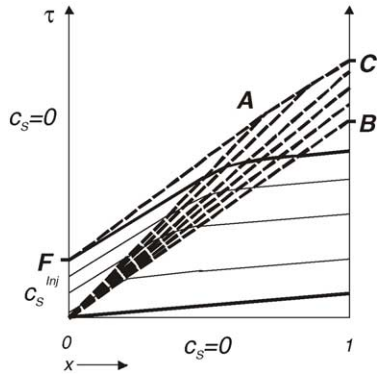

Fig. 9. Case (a), dashed lines: modifier characteristics; solid lines: solute characteristics.

$$\left.\frac{\mathrm{d}\tau}{\mathrm{d}x}\right|_{\mathrm{S}} = 1 + \nu^* H_{\mathrm{S}}(c_{\mathrm{M}}) \tag{22}$$

Using Eq. (15), the modifier concentration in the wave region is known as a function of τ and x:

$$c_{\mathrm{M}} = \frac{1}{K_{\mathrm{M}}}\left(\sqrt{\frac{H_{\mathrm{M}}\nu^* x}{\tau - x}} - 1\right) \tag{23}$$

Substituting Eq. (23) into Eq. (22), and using the functional dependence of H_{S} on c_{M}, one can integrate Eq. (22) numerically, thus obtaining for instance the characteristics illustrated in Fig. 9, It has to be noted for the following figures, that dashed lines represent modifier characteristics, thick solid lines the boundaries of the region where solute is present and thin solid lines the solute characteristics.

It can be readily seen that the solute peak at the column outlet is broader than the injected pulse. This case is very similar to the linear case (a) in Section 2.1.

Case (b) has to be divided into two sub-cases, whether $\sigma_{\mathrm{S}}(c_{\mathrm{M}}^0) < \sigma_{\mathrm{M}}^{\mathrm{F-A}}$ (case b1) or $\sigma_{\mathrm{S}}(c_{\mathrm{M}}^0) > \sigma_{\mathrm{M}}^{\mathrm{F-A}}$ (case b2). In the former case, the solute characteristics hit the line F–A and the solute accumulates into a sharp peak at the rear end of the modifier peak, with a behavior similar to that of the linear case (c) in Section 2.1. When the solute peak passes point A and migrates on line A–C, the slope of the solute characteristics on the rear end of the modifier peak decreases due to the decreasing height of the peak. Therefore, it may become lower than the local slope of line A–C and may leave the shock, thus entering the dispersive wave as in case (a). The local slope for a point P with concentration $c_{\mathrm{M}}^{\mathrm{P}}$ on line A–C is given by

$$\left.\frac{\mathrm{d}\tau}{\mathrm{d}x}\right|_{\mathrm{M}}^{\mathrm{A-C}} = 1 + \nu^* \frac{H_{\mathrm{M}}}{(1 + K_{\mathrm{M}} c_{\mathrm{M}}^0)(1 + K_{\mathrm{M}} c_{\mathrm{M}}^{\mathrm{P}})} \tag{24}$$

and with Eq. (22), the necessary condition for the solute peak leaving the shock at point P can be written as:

$$H_{\mathrm{S}}(c_{\mathrm{M}}^{\mathrm{P}}) \le \frac{H_{\mathrm{M}}}{(1 + K_{\mathrm{M}} c_{\mathrm{M}}^0)(1 + K_{\mathrm{M}} c_{\mathrm{M}}^{\mathrm{P}})} \tag{25}$$

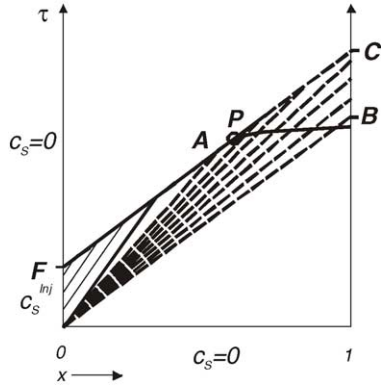

Fig. 10. Case (b1), dashed lines: modifier characteristics; solid lines: solute characteristics.

Fig. 10 illustrates such a situation in the physical plane. If inequality Eq. (25) is on the contrary never fulfilled on line A–C, the solute peak will elute together with the rear end of the modifier peak leading to a chromatogram similar to that of Fig. 7.

For case (b2), the solute characteristics are not confined to the peak rear since the slope at c_{M}^0 is larger than that of line F–A. Therefore, the solute peak and the modifier perturbation split up and travel independent of each other, as in the linear case (b) of Section 2.1 (see Figs. 4 and 5).

In case (c), the slope of the solute characteristics is intermediate between the slope of line 0–A and that of F–A. Therefore, some solute characteristics intersect line 0–A and proceed as in case (a), whereas others intersect line F–A and proceed as in case (b). The fraction $\gamma_{0-\mathrm{A}}$ of lines crossing line 0–A, which is proportional to the amount of solute traveling through the dispersive wave front, can be calculated as:

$$\gamma_{0-\mathrm{A}} = \frac{\tau_{\mathrm{A}} - \sigma_{\mathrm{S}}(c_{\mathrm{M}}^{\mathrm{Inj}})x_{\mathrm{A}}}{\tau_{\mathrm{Inj}}} \tag{26}$$

An example of the column dynamics corresponding to case (c) is illustrated in Fig. 11. It can be seen, that some of

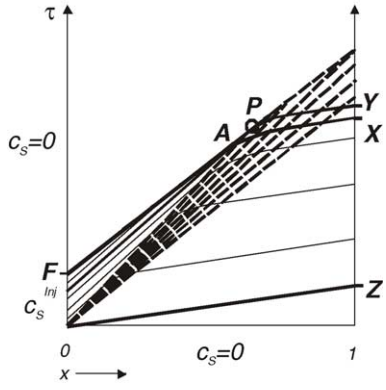

Fig. 11. Case (c), dashed lines: modifier characteristics; solid lines: solute characteristics.

Fig. 12. Case (c), double peak chromatogram.

the characteristics leave the plateau region 0–A–F through line 0–A, while the solute hitting line F–A travels as a sharp peak, crosses point A and leaves the shock at a point P, as discussed. Between point A and P, no solute is present, and so is in the region between lines A–X and P–Y. This leads to a solute chromatogram (Fig. 12) exhibiting two peaks, a first one resulting from the solute crossing line 0–A and being eluted between Z and X with a low solute concentration as discussed in Section 2.1 and a second sharp peak being eluted at Y. The ratio of the peak areas of the first and the second peak is given by Eq. (26).

This analysis can be extended to discuss and explain distorted peaks. Let us consider the case where point A in Fig. 11 does not exist, i.e. it is located beyond $x = 1$. This occurs when τ_{Inj} is sufficiently large. As a consequence, the modifier plateau concentration $c_{\mathrm{M}}^{\mathrm{Inj}}$ is present until the column outlet. In this case the solute chromatogram would consist of three parts: a broad, low concentration peak from the solute crossing the front of the injected modifier pulse; a peak at the injected pulse concentration; a very sharp peak from the solute eluting with the rear of the modifier peak. An example of this kind of chromatogram is illustrated in Fig. 13. One can easily imagine that band-broadening in real columns leads in this case to a chromatogram that looks similar to that obtained for an anti-Langmuir isotherm.

The observation has indeed been reported based on experimental data [12]; this situation will be further analyzed through simulations in the next section.

For the case of a positive modifier perturbation, the peak travels with a shock front and a dispersive wave rear end [9]. Since the treatment and the different cases are exactly analogous to those already discussed for a negative modifier perturbation, these will not be pursued any longer.

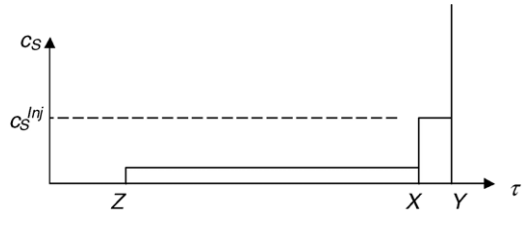

Fig. 13. Case (c), distorted peak diagram.

3. Dispersive model simulations

An equilibrium-dispersive model was used in order to verify the results obtained from equilibrium theory and to get a more realistic picture (i.e. including dispersive effects) of the behavior of these systems, with specific attention on the phenomena of peak broadening, peak distortion and double peaks.

The following mass balances of the modifier and the solute constituting the classical equilibrium dispersive model were discretized in space and integrated in time using the DIVPAG-routine from the IMSL library.

$$\frac{\partial c_{\mathrm{M}}}{\partial x} + \left(1 + \nu^* \frac{H_{\mathrm{M}}}{(1 + K_{\mathrm{M}} c_{\mathrm{M}})^2}\right) \frac{\partial c_{\mathrm{M}}}{\partial \tau} = \frac{\varepsilon_{\mathrm{b}}}{\varepsilon^*} D_{\mathrm{eff}} \frac{\partial^2 c_{\mathrm{M}}}{\partial x^2} \frac{1}{uL} \tag{27}$$

$$\frac{\partial c_{\mathrm{S}}}{\partial x} + (1 + \nu^* H_{\mathrm{S}}(c_{\mathrm{M}})) \frac{\partial c_{\mathrm{S}}}{\partial \tau} + \nu^* c_{\mathrm{S}} \frac{\mathrm{d}H_{\mathrm{S}}(c_{\mathrm{M}})}{\mathrm{d}c_{\mathrm{M}}} \frac{\partial c_{\mathrm{M}}}{\partial \tau} = \frac{\varepsilon_{\mathrm{b}}}{\varepsilon^*} D_{\mathrm{eff}} \frac{\partial^2 c_{\mathrm{S}}}{\partial x^2} \frac{1}{uL} \tag{28}$$

The number of grid points was chosen large enough to guarantee the convergence of the numerical method. The simulation parameters used are summarized in Table 1.

In the following we consider a few examples that have been selected among those where the equilibrium theory analysis reported in the previous chapter indicates a major difference with respect to the behavior of an isocratic pulse.

At first, we consider detailed simulations for case (a) as defined in Section 2.2, enforcing the following operation conditions: $c_{\mathrm{M}}^{\mathrm{Inj}} = 8.7\,\mathrm{g/l}$, $c_{\mathrm{M}}^{0} = 9.3\,\mathrm{g/l}$ and $\tau_{\mathrm{Inj}} = 0.2$. The solid line in Fig. 14 shows the resulting chromatogram. In comparison to the isocratic peak (dashed line in Fig. 14) one observes a significant broadening of the solute peak due to the interaction of the modifier and the solute peak, as predicted by equilibrium theory (c.f. Fig. 9).

In order to verify the predictions made for case (b1), the operating conditions were chosen as $c_{\mathrm{M}}^{\mathrm{Inj}} = 7\,\mathrm{g/l}$, $c_{\mathrm{M}}^{0} = 12\,\mathrm{g/l}$ and $\tau_{\mathrm{Inj}} = 0.12$. The detailed simulation shown in Fig. 15 confirms both the increase of the retention time as well as the peak sharpening effect due to the sample–solvent interaction, as illustrated in Fig. 10.

Table 1
Simulation parameters

d_{ax} [cm]	0.003
u [cm/min]	1
ε^*	0.65
ε_{B}	0.4
ν^*	0.538
Grid points	5000
$H_{\mathrm{S}}(c_{\mathrm{M}})$	8.43×10^{11} (c_{M} [g/l])$^{-12.52}$
H_{M}	3.18
K_{M} [l/g]	0.0363
L [cm]	10

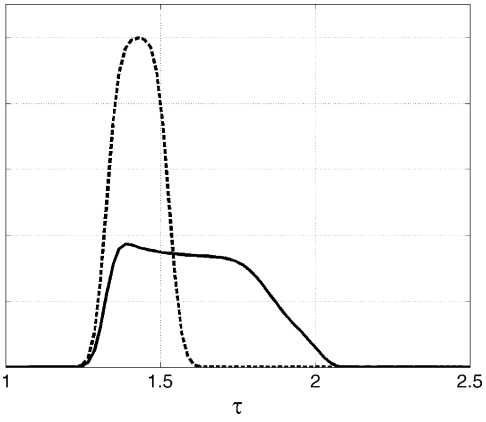

Fig. 14. Dispersive model simulations, case (a); solid line: solute chromatogram; dashed line: isocratic solute peak.

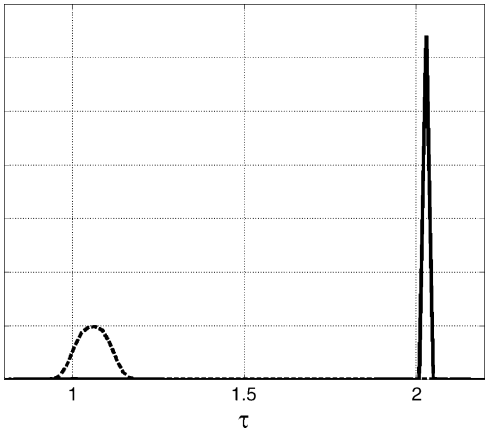

Fig. 15. Dispersive model simulations, case (b1); solid line: solute chromatogram; dashed line: isocratic solute peak.

The next example is concerned with the occurrence of double peaks and the effect of varying injection volumes. The simulated chromatograms for $c_M^{Inj} = 8.54$g/l, $c_M^0 = 10$ g/l and various injection times are shown in Fig. 16 while the last two columns in Table 2 contain the retention times of the peaks which were taken at the peak maximum.

It is seen in Fig. 16, that the dispersive model predicts only one peak in the chromatogram for small injection volumes ($\tau_{Inj} = 0.01$). For increasing injection volumes, the effect of the modifier perturbation in the dispersive model simulation becomes more significant and a second peak occurs. While

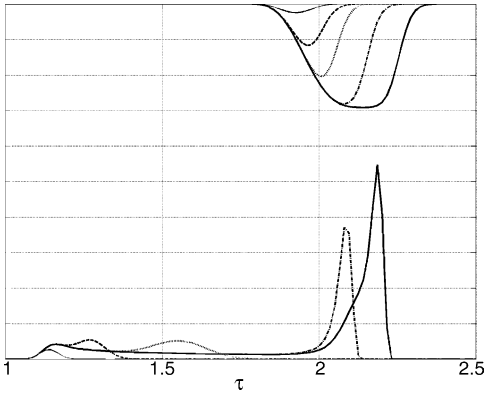

Fig. 16. Dispersive model simulations, solute and modifier chromatograms; thin solid lines: $\tau_{Inj} = 0.01$; dashed lines: $\tau_{Inj} = 0.05$; dotted lines: $\tau_{Inj} = 0.1$; dash-dotted lines: $\tau_{Inj} = 0.2$; thick solid lines: $\tau_{Inj} = 0.3$.

the retention time of the first peak is constant with increasing injection volumes, the elution time of the second peak becomes larger. For the largest injection volume ($\tau_{Inj} = 0.3$), the second solute peak containing the major portion of the injected solute shows an anti-Langmurian shape as explained in Section 2.2, case (c), in the context of Fig. 13.

Indeed, the chosen operating parameters belong to case (c) and, as already discussed there, double peaks and distorted peaks are predicted by equilibrium theory. The results of the equilibrium theory model are reported in the first four columns of Table 2 which contain the retention times from the equilibrium theory model τ_Z, τ_X, τ_Y (columns 1–3) as described with reference to Figs. 12 and 13 while the fourth column indicates the x-position of point A (c.f. Fig. 10). It has to be noted that rows with no entries in the fourth column of Table 2 indicate that point A is non-existent and therefore, the modifier concentration in the injection, c_M^{Inj}, is present at the column outlet and a chromatogram as in Fig. 13 is expected while for $\tau_{Inj} = 0.01$, the point A is present inside the column and two separate peaks as in Fig. 12 are predicted.

The problem, that the chromatogram from the dispersive model shows only one peak for the short injection time $\tau_{Inj} = 0.01$, while two are foreseen by equilibrium theory, is due to the fact that the modifier perturbation is very small and flattens out due to the dispersion close to the inlet of the column. The predicted retention time from the dispersive model as reported in Table 2 is indeed the same as the one

Table 2
Comparison of retention times from equilibrium theory and dispersive model simulations

	Equilibrium theory results (c.f. Figs. 12 and 13)				Retention time τ (at peak maximum) dispersive model	
	τ_Z	τ_X	τ_Y	x_A	1st peak	2nd peak
$\tau_{Inj} = 0.01$	1.14	1.38	1.39	0.26	1.14	–
$\tau_{Inj} = 0.05$	1.14	2.00	2.01	–	1.16	1.27
$\tau_{Inj} = 0.1$	1.14	2.00	2.06	–	1.16	1.55
$\tau_{Inj} = 0.2$	1.14	2.00	2.16	–	1.16	2.08
$\tau_{Inj} = 0.3$	1.14	2.00	2.26	–	1.16	2.19

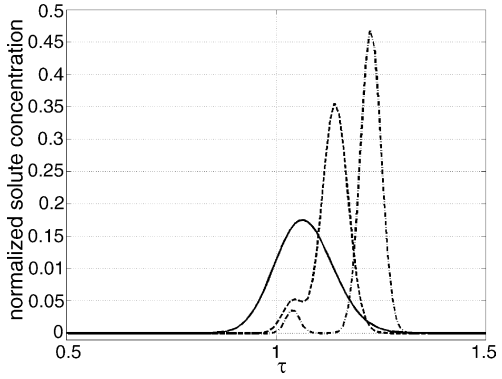

Fig. 17. Dispersive model simulations, role of axial dispersion; solid line: $d_{ax} = 3 \times 10^{-2}$ cm; dashed line: $d_{ax} = 3 \times 10^{-3}$ cm; dash-dotted line: $d_{ax} = 3 \times 10^{-4}$ cm.

of the isocratic peak calculated from equilibrium theory, i.e. $\tau = 1.14$.

For the larger injection times, i.e. above $\tau_{Inj} = 0.01$, it can be seen from Table 2 that the retention times of the second solute peak calculated using the dispersive model simulation approach those from equilibrium theory, i.e. the rectangular peak between τ_X and τ_Y. This can be explained by the fact that the impact of dispersion on the shape of the modifier peak becomes smaller with increasing modifier peak size, i.e. with increasing injection times.

Furthermore, we see from Table 2 that the first solute peak in the dispersive model chromatogram is approximately eluted at the retention time of an isocratic peak, $\tau = 1.14$, which indicates that it propagated in the column as predicted by equilibrium theory (c.f. Fig. 11, line 0–Z) and therefore, is identical with τ_Z.

Let us now consider the impact of different axial dispersion coefficients for a given injection time. The results as shown in Fig. 17 were obtained through dispersive model simulations using $\tau_{Inj} = 0.03$, $c_M^{Inj} = 8$ g/l and $c_M^0 = 11$ g/l.

For these conditions the equilibrium theory predicts a very sharp peak at $\tau = 1.67$ while the isocratic equilibrium theory peak is eluted at $\tau = 1.06$. For large axial dispersion coefficients, the modifier peak is flattened out fast and therefore its effect on the solute peak is lower. With decreasing axial dispersion coefficients, the impact of the modifier peak on the solute peak becomes more pronounced since the modifier perturbation proceeds longer along the column for smaller dispersion coefficients. Hence, in Fig. 17 we observe a small hump which is eluted always at the same time, in fact being the retention time belonging to the solute Henry coefficient at the eluent modifier concentration (i.e. the isocratic retention time, $\tau = 1.06$) and a larger peak which detaches from the first hump sooner for decreasing axial dispersion coefficients. The retention time of the second peak increases with smaller axial dispersion. In the limit of an infinite number of stages, this approaches the retention time predicted by equilibrium theory, i.e. $\tau = 1.67$.

4. Interpretation of experimental data

The treatment of sample–solvent induced phenomena presented above can be used to analyze and explain some literature experimental results about retention time measurements of the peptide *n*-formyl-Met-Phe in water-acetonitrile mixtures on a Novopak C_{18} column [13]. The modifier concentration in the eluent stream was varied between 10 and 60 vol.% acetonitrile, and *n*-formyl-Met-Phe was injected using a sample solvent containing 20 vol.% acetonitrile. The squares in Fig. 18 indicate the values of the Henry coefficients calculated from the measured retention times as a function of the acetonitrile concentration using the standard relationship for isocratic chromatography. The thick solid curve in the same figure represents the fitting of the experimental data (see inset in Fig. 18) which has been obtained using a typical exponential correlation for the Henry coefficient of *n*-formyl-Met-Phe as a function of the acetonitrile concentration (c.f. row 3 in Table 3). In the original work it was observed that significant deviations from the relation above are observed at the higher acetonitrile concentration values. However, this discrepancy is an artifact due to the sample–solvent induced modifier–solute interaction discussed in this work and can be interpreted correctly using the equilibrium theory results reported above.

In Section 2.2 we have shown that the interaction between the modifier and the solute peak depends strongly on the relative magnitude of $\sigma_S(c_M^{Inj})$ with respect to σ_M^{0-A} and σ_M^{F-A}. These three quantities can be computed using Eq. (16), (17) and (21) and the experimental parameter values summarized in Table 3. The obtained values are shown in Fig. 19 as a function of the eluent modifier concentration together with the slope of the solute characteristic at the eluent modifier concentration $\sigma_S(c_M^0)$.

From Fig. 19, it can be seen that if the eluent modifier concentration c_M^0 is between 20% and approximately 44-vol.% acetonitrile, we have $\sigma_S(c_M^{Inj}) > \sigma_M^{0-A}$ and $\sigma_S(c_M^0) > \sigma_M^{F-A}$, and therefore case (b2) applies and a low interference between the modifier and the solute peak is expected from equilibrium theory. Instead for modifier concentrations above approximately 44-vol.%, case (b1) applies since $\sigma_S(c_M^{Inj}) > \sigma_M^{0-A}$ and $\sigma_S(c_M^0) < \sigma_M^{F-A}$ and from the insights gained in Section 2.2, a strong distortion of the retention time is expected.

Table 3
System parameters for *n*-formyl-Met-Phe from Kim et al. [13]

c_M^{Inj} [vol.%]	20
ν^*	0.46
$H_S(c_M$ [vol.%])	$\frac{1}{\nu^*}(1090e^{-0.369c_M} + 41.1e^{-0.129c_M})$
H_M [(l/g)/(l/g)]	1.14
K_M [l/g]	0.15
V_{Inj} [μl]	20
$\dot{V}$[ml/min]	1
V_{column} [ml]	1.792

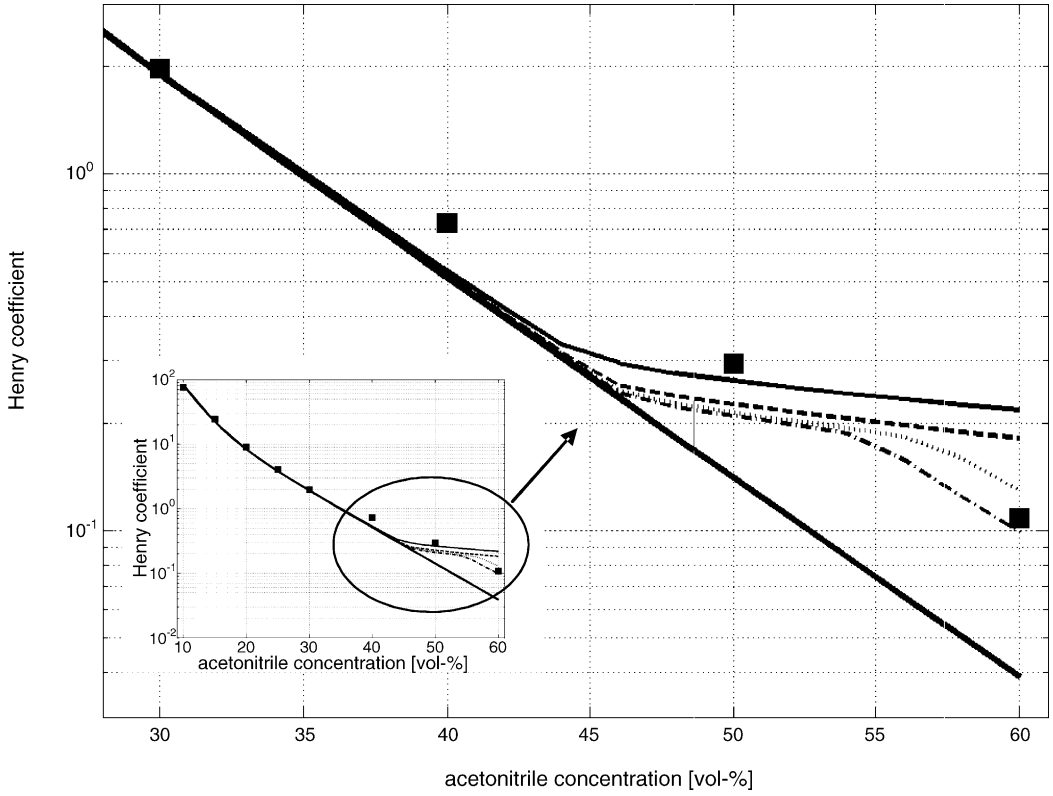

Fig. 18. Comparison of experimental data and correlation; thick solid line: exponential correlation for Henry coefficient; squares: Henry coefficients computed from measured retention times assuming isocratic conditions; thin lines: Henry coefficients computed from retention times obtained from equilibrium theory accounting for the sample–solvent induced modifier–solute interactions: $\tau_{Inj} = 0.01$ (solid), $\tau_{Inj} = 0.003$ (dashed), $\tau_{Inj} = 0.0015$ (dotted), $\tau_{Inj} = 0.001$ (dash-dotted).

For both cases identified above, we can compute the retention time, τ_S, predicted by the equilibrium theory using the corresponding equations from Section 2.2, i.e. Eqs. (16) and (17) and Eqs. (21)–(23).

Using these retention times τ_S as experimental values, we can compute the so-called "apparent" Henry coefficients, H_S, using the isocratic equation $H_S = (\tau_S - 1)/\nu^*$. The resulting values of the "apparent" Henry coefficients are shown in Fig. 18 as a function of the eluent modifier concentration for various dimensionless injection times, τ_{Inj}. It is worth noting that the injection volume used by Kim et al. [13] converts into a dimensionless injection time of $\tau_{Inj} = 0.016$. Note that in calculating the retention times, τ_S, the value of the Henry coefficient has been taken from the exponential function reported in Table 3, which corresponds to the thick curve in Fig. 18.

From the results in Fig. 18 it is seen that for all modifier concentrations up to approximately 44 vol.%, the calculated retention times τ_S lead to "apparent" Henry coefficients H_S which are very close to the actual ones given by the exponential correlation. But for concentrations larger than 44 vol.%, the "apparent" Henry coefficients H_S deviate significantly from the real ones and approach those measured experimentally. This clearly indicates that such a deviation is not due to inaccuracies of the exponential correlation but it is due to the influence of the sample–solvent interaction.

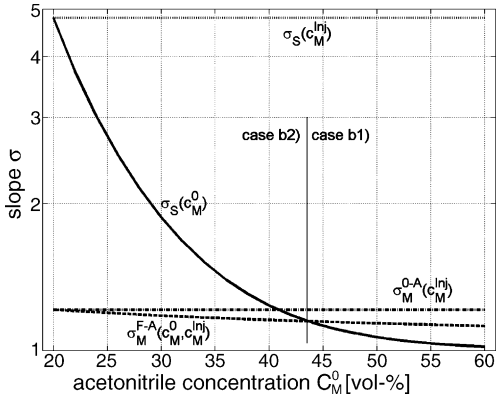

Fig. 19. Slopes of characteristics in the physical plane as function of acetonitrile concentration c_M^0 for *n*-formyl-Met-Phe; solid line: slope of solute characteristics in state 0, $\sigma_S(c_M^0)$; dash-dotted line: slope of modifier characteristic 0–A, $\sigma_M^{0-A}(c_M^{Inj})$; dashed line: slope of modifier characteristic F–A, $\sigma_M^{F-A}(c_M^0, c_M^{Inj})$; dotted line: slope of solute characteristic at state inj, $\sigma_S(c_M^{Inj})$.

5. Guidelines to avoid retention time distortion

As stated in the introduction, sample–solvent induced modifier–solute interactions can be avoided by simply using a modifier concentration in the sample solvent equal to the

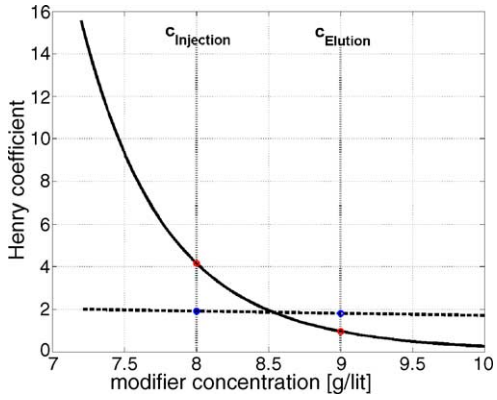

Fig. 20. Adsorptive properties of solute and modifier; solid line: $H_S(c_M^0)$; dashed line: $H_M/((1+K_M c_M^0)(1+K_M c_M^{Inj}))$ and $H_M/(1+K_M c_M^{Inj})^2$.

one in the eluent. For the cases where this is not possible, we develop in the following general guidelines to minimize such interactions. As seen previously, a helpful figure for the analysis of sample–solvent induced phenomena is the plot of the slopes of the characteristics, $\sigma_M^{F-A}(c_M^0, c_M^{Inj})$, $\sigma_M^{0-A}(c_M^{Inj})$, $\sigma_S(c_M^{Inj})$ and $\sigma_S(c_M^0)$, as a function of the modifier concentration c_M^0. Since these slopes are linear functions of $H_M/((1+K_M c_M^0)(1+K_M c_M^{Inj}))$, $H_M/(1+K_M c_M^{Inj})^2$, $H_S(c_M^{Inj})$ and $H_S(c_M^0)$, respectively, we can plot these values instead as shown in Fig. 20 for the system whose parameters are summarized in Table 1.

It has to be noted, that the functions $H_M/((1+K_M c_M^0)(1+K_M c_M^{Inj}))$ and $H_M/(1+K_M c_M^{Inj})^2$ yield nearly the same values and hence they can not be distinguished in Fig. 20.

We have seen that in order to avoid strong interactions of the solute and the modifier peak, a large difference in the slope of the characteristics of the solute in the sample–solvent and the modifier peak is desired so as that the two separate as fast as possible and so their interaction vanishes. By considering the data in Fig. 20, this leads to the conclusion that the modifier concentration in the injection volume should therefore be as far as possible from the intersection and preferably on the left side of the latter, since the largest difference can be obtained there. As a second point we should consider that the solute in the injection has to enter sooner or later the region containing the eluent modifier concentration. If the injection and elution modifier concentration are on different sides of the intersection, the solute has to cross a state where it travels as fast as the modifier peak which always causes severe retention time distortion. This leads to the conclusion that it is desirable that the injection and the eluent modifier concentration are on the same side of the intersection.

In summary, two general guidelines to minimize the effect of sample–solvent induced modifier–solute peak interaction can be derived: the injection modifier concentration should be far away from the intersection, preferably on the left side, and the eluent and injection modifier concentrations should be on the same side of the intersection.

6. Conclusions

The generic difference between system peaks and sample–solvent induced phenomena has been discussed. The latter occurs when the modifier concentration in the sample–solvent is not the same as in the eluent, while the former one occurs when the modifier adsorption is affected by the presence of the solute. These interactions have been analyzed in detail using an equilibrium theory model solved by the method of characteristics, assuming a linear isotherm for the solute and both a linear or a Langmuir isotherm for the modifier. All possible operating conditions have been divided into different cases and three main types of behavior have been identified, including peak broadening, sharpening and distortion as well as double peaks. The results of the equilibrium theory model have been verified using a numerical simulation based on an equilibrium-dispersive model. It has been found, that in the case where the Henry constant of the solute is estimated from experimental measurements of the retention time obtained using a different modifier concentration in the injection and in the eluent, severe errors can be made when the sample–solvent induced modifier–solute interactions are not accounted for. In particular, based on the results of the analysis using equilibrium theory, the experimental Henry constants of a peptide previously reported in the literature as a function of the modifier concentration have been interpreted and corrected. General guidelines have been provided about how to avoid such dangerous situations.

7. Nomenclature

c_i	liquid phase concentration of component i
d_{ax}	effective axial dispersion number
$D_{eff} = d_{ax}u$	effective axial dispersion coefficient
H_i	Henry coefficient of component i
K_i	selectivity of component i
L	column length
q_i	solid phase concentration of component i
t	time
u	superficial velocity
$x = z/L$	dimensionless space coordinate
z	space coordinate

Greek symbols

$\varepsilon^* = \varepsilon_B + (1-\varepsilon_B)\varepsilon_P$	total column porosity
ε_B	bed porosity
ε_P	particle porosity
γ	fraction of solute as defined in Eq. (26)
$\nu^* = (1-\varepsilon^*)/\varepsilon^*$	phase ratio

σ_i slope of characteristic in physical plane of component i

$\tau = ut/(L\varepsilon^*)$ dimensionless time

Superscripts and subscripts

0	state 0
Inj	state injection
M	modifier
Out	state at column outlet
S	solute

References

[1] T. Fornstedt, G. Guiochon, Anal. Chem. 66 (1994) 2686.
[2] S. Golshan-Shirazi, G. Guiochon, Anal. Chem. 62 (1990) 923.
[3] S. Golshan-Shirazi, G. Guiochon, Anal. Chem. 61 (1989) 2373.
[4] W. Feng, X. Zhu, L. Zhang, X. Geng, J. Chromatogr. A 729 (1996) 43.
[5] K.J. Williams, A. Li Wan Po, W.J. Irwin, J. Chromatogr. 194 (1980) 217.
[6] D. Vukmanic, M. Chiba, J. Chromatogr. 483 (1989) 189.
[7] P. Jandera, G. Guiochon, J. Chromatogr. 588 (1991) 1.
[8] G. Guiochon, S. Golshan-Shirazi, A.M. Katti, Fundamentals of Preparative and Nonlinear Chromatography, Academic Press, Boston, etc., 1994.
[9] H.-K. Rhee, R. Aris, N.R. Amundson, First-order Partial Differential Equations, Volume 1: Theory and Application of Single Equations, Dover Publications, New York, 2001.
[10] H.-K. Rhee, R. Aris, N.R. Amundson, First-order Partial Differential Equations, Volume 2: Theory and Application of Hyperbolic Systems of Quasilinear Equations, Dover Publications, New York, 2001.
[11] G. Ströhlein, H.-K. Rhee, M. Mazzotti, M. Morbidelli. Modeling of sample–solvent induced modifier–solute peak interactions in chromatography, AIChE J. (2005) in press.
[12] S. Golshan-Shirazi, G. Guiochon, J. Chromatogr. 461 (1989) 1.
[13] B. Kim, A. Velayudhan, J. Chromatogr. A 796 (1998) 195.